<u>Solar Position</u>

Firstly the sun position is calculated. The sun position algorithm calculates the sun position in two forms: first as a unit vector extending from the Cartesian origin toward the sun, and second as azimuthal and altitudinal angles. The algorithm relies on the latitude, longitude and time zone offset from UTC in order to determine the position of the sun at every time step throughout the year.

The equations used are:

$$t_{solar} = 4(L_{st} - L_{loc}) + E + t_{standard}$$

Where:

$$L_{st} = tz_{offset} * 15$$

$$E = 229.2(0.000075 + 0.001868 * \cos B - 0.0320077 * \sin B - 0.014615 * \cos 2B - 0.04089 * \sin 2B)$$

L_{st} is the local standard meridian, L_{loc} is the given longitude and E is the equation of time, in minutes.

The solar time can then be used to calculate the Hour angle, ω:

$$\omega = \Delta t_{noon} * 15$$

Where Δt_{noon} is the difference between solar time and solar noon.

Once the declination, δ is known, the solar zenith and azimuthal angle of the sun can be found:

$$\delta = 23.45 * \sin\left(360 * \frac{284 + n}{365}\right)$$

$$\theta_z = \cos^{-1}(\cos \varphi * \cos \delta * \cos \omega + \sin \varphi * \sin \delta)$$

$$\gamma_s = sign(\omega)\left|\cos^{-1}\left(\frac{\cos \theta_z \sin \phi - \sin \delta}{\sin \theta_z \cos \phi}\right)\right|$$

Where:

- n is the day of the year (1 to 365)
- θ_z is the sun zenith angle (subtract from 90 to get the altitude angle, θ_a)
- φ is the given latitude
- γ_s is the sun azimuthal angle

The sun altitude and azimuth can be converted to unit vector components as follows:

$$\vec{s_i} = \cos \theta_a * \sin \gamma_s$$

$$\vec{s_j} = \cos \theta_a * \cos \gamma_s$$

$$\vec{s_k} = \sin \theta_a$$

Reflected Sun Vector

$$x_1' - x_0 = v - 2(v \cdot \hat{n})\,\hat{n}$$

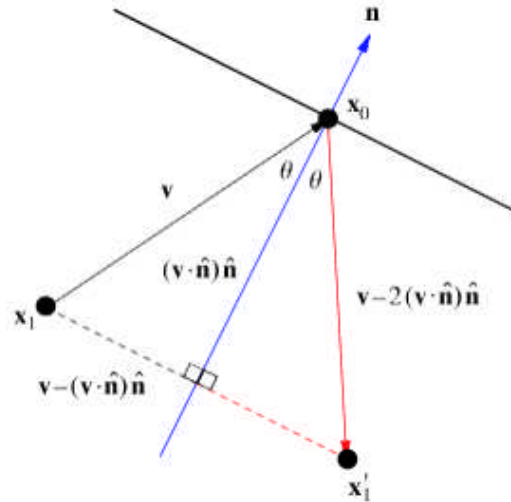Figure 1 illustrates this vector reflection graphically.

Figure 1 - Vector reflection over normal vector of plane. Source: mathworld.wolfram.com/Reflection.html

Scattering and Subtended Beam Angle

The reflected sun vector calculated above defines the axis of a conical beam which represents an actual beam of sunlight. This sun beam is translated to extend from the observation point (OP) toward the PV array (note this is the whole array not an individual panel). The aperture of this sun beam is equivalent to the subtended beam angle. This is formed of the sum of the sun shape and an additional scattering caused by slope error. This additional scattering takes into account errors in the panel angle across the array and slightly widens the subtended beam angle. The calculation is as follows:

$$\beta = 2 * \left(\frac{\theta_{sun\ angle}}{2} + 2 * 3 * \theta_{slope\ error} \right)$$

Beam Projection onto the PV Array Plane

This calculation takes the sun beam angle defined above and uses the result to calculate a cone from the eye back out to the array in order to define how much of the array is potentially visible and the intensity of any reflections.

The calculation is carried out in several steps. Firstly points lying on the edge of the beam in a conical section orthogonal to the axis (the subtended beam angle) are calculated. This conical section is arbitrarily defined to be 1 meter from the cone apex (the OP).

These 30 points are calculated by randomly generating two coordinates and solving for the third using the following equation:

$$v_{axis} \cdot v_{radius} = 0$$

This equation states that the cone axis is orthogonal to the radius vectors of the conical section upon which the 30 conical points lie. Next, conical edge vectors are defined by subtracting the cone apex (the OP) from the cone points. This collection of vectors extends from the OP toward the PV array plane.

These vectors define the conical sun beam. At their centre, or the axis of the cone, is the reflected sun vector calculated above. These conical vectors are then intersected with the PV array plane. This cone-plane intersection will be an elliptical conical section defined by 30 co-planar points. These intersection points are calculated using line-plane intersection equations:

$$d = \frac{(p_0 - I_0) \cdot \vec{n}}{I \cdot \vec{n}}$$

$$(x, y, z) = dI + I_0$$

Where:

- $\vec{n}$ is the PV array panel normal vector

- I is one of the vectors extending from the OP to the PV array plane, which define the conical sun beam.

- I_0 is a point on the vector (the OP)

- p_0 is a point on the PV array plane

- d is the distance from the OP to the intersection point, and

- (x, y, z) define the intersection point for this vector.

The n intersection points found using the above equations define the elliptical conical section of the sun beam cone as it intersects the PV array plane. Glint is present when any of the OP vertices lie within this co-planar elipse.

In more simple terms we have calculated a cone defining the glint from the array (sections 2 and 3). When an observation point (OP) falls within this cone the subtended angle (the axis)

is used to define a cone from the viewer's eye back to the array. Where this cone intersects then glint will be received by the viewer. The amount of intersection is then used in the intensity calculation and also defines the subtended angle. Both of these are then used to calculate the potential for after-image.

Direct Normal Irradience (DNI), Reflectance and Subtended Beam Angle

The software modifies the peak DNI for a clear day irradiance profile. This lowers the DNI in the morning and evenings around the noon value which is calculated based upon the results of section 1 above. The calculation is as followed:

$$DNI = \cos(1 - t_s)$$

Here t_s represents the normalized time relative to solar noon. Normalization is based on the amount of time between sunrise or sunset and solar noon. Sandia determined the DNI scaling profile by fitting empirical DNI data to the cosine function, as illustrated in Figure 4. Note that DNI on any given day can be affected by cloud cover, atmospheric attenuation, and other environmental factors.
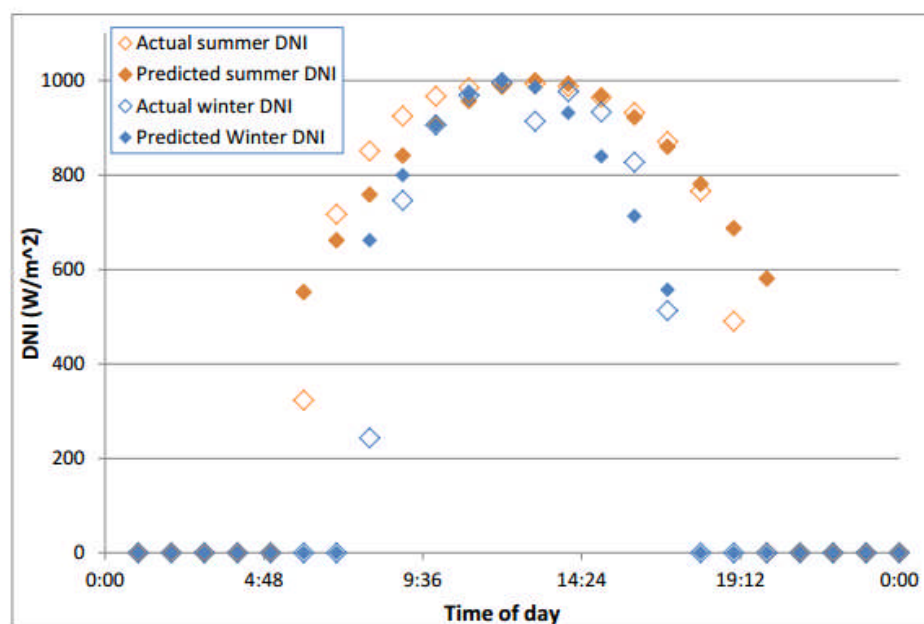

Figure 4 - Fit functions modeling normalized DNI vs. hour. Cosine was chosen to profile empirical data.

The DNI is further modified by Panel reflectivity which can be varied for each time step to account for the position of the sun relative to the array.

Smooth glass and light textured glass with and without Anti-Reflection coating, along with deeply textured glass were analysed to derive accurate functions for computing reflectivity based on sun incidence angle.

Table 1 contains the fit functions for different panel reflectivities.

Table 1 - Reflectance fit functions for PV cover types.

PV Glass Cover Type	Fit Function Defined over $0° \leq \theta \leq 60°$	Fit Function Defined over $60° < \theta < 90°$
Smooth Glass without Anti-Reflection Coating	$y = 1.1977E\text{-}5\ x^2 - 9.5728E\text{-}4\ x + 4.410E\text{-}2$	$y = 6.2952E\text{-}5\ e^{0.1019x}$
Smooth Glass with Anti-Reflection Coating	$y = 1.473E\text{-}5\ x^2 - 9.6416E\text{-}4\ x + 3.2395E\text{-}2$	$y = 4.7464E\text{-}5\ e^{0.1051x}$
Light Textured Glass without Anti-Reflection Coating	$y = 1.5272E\text{-}5\ x^2 - 1.1304E\text{-}3\ x + 4.305E\text{-}2$	$y = 7.3804E\text{-}5\ e^{0.0994x}$
Light Textured Glass with Anti-Reflection Coating	$y = 1.4188E\text{-}5\ x^2 - 1.0326E\text{-}3\ x + 3.9016E\text{-}2$	$y = 7.0179E\text{-}5\ e^{0.0994x}$
Deeply Textured Glass	$y = 6.8750E\text{-}6\ x^2 - 6.5250E\text{-}4\ x + 2.10E\text{-}2$	$y = 4.1793E\text{-}5\ e^{0.0834x}$

The glare analysis must account for the actual visible area of the PV array when viewed from the observation point. For example, less viewable area will be apparent when viewing an array with panel tilt of 0 degrees on a flat surface from the side than when viewing it from above in an aircraft.

To account for this, the analysis replaces the solar beam angle with an array-limiting beam angle if the latter is a smaller value. This represents the physical situation where the sun beam "overflows" the PV array from the viewer's perspective, and thus less glare is possible.

The calculation is as follows:

$$\theta = \frac{1}{d}\sqrt{\frac{4 * A * \left|\cos \theta_{ref-pva}\right|}{\pi}}$$

where:

- A is area of PV array

- d is distance between observer and array

- $\theta_{ref\text{-}pva}$ is angle between reflected sun vector and PV array normal

Methodology Limitations

There are some identified limitations with the methodology used that should be noted and accounted for when considering the content of the subsequent analysis.

ZTV & GGZ Limitations

The ZTV is based upon NASA SRTM V3 data which represents bare earth topography. Although the ZTV does take into account screening from an intervening land form, it does not take into account any potential screening from obstacles such as trees, hedgerows or buildings.

Furthermore, the ZTV is a binary classification based upon visibility of any section of the solar farm. For example, there is no distinction between being able to see 1 solar panel or the entire array. This is crucial when considering the GGZ. For example, a receptor may be in the northern extent of the GGZ and may be within the ZTV as a result of the southerly panels in the array being visible. In this instance the analysis may indicate that glint is visible when in fact glint would not be visible as receptors in the northern extents of the GGZ may not receive glint from the southerly panels in the array.

The ZTV is based on a number of representative observation points along and within the site boundary. It is possible that a receptor may not be included within the ZTV as a consequence of a part of the site being visible that isn't included as an observation point. This is however considered highly unlikely.

Computer Simulation

The GlareGuage software tool is used primarily for assessing the potential impacts of glint on aviation receptors - both aircraft and control towers. As such it does provide something of a worst case scenario, modelling a situation where any glint could potentially occur rather than where glint might be most expected to cause an issue in reality.

Additionally, it is important to consider some of the other limitations of the modelling software that has been used.

One such limitation is that the model does not account for any screening from other panels within the solar farm. It assumes that glint is possible from every point within the array boundary and does not account for the panel in front screening glint from the panel behind. Again this does provide a worst case scenario and, particularly in the case of an aircraft flying overhead, is a perfectly reasonable approach but in the case of a ground receptor it does represent quite a large potential for over estimation within the model.

Another limitation is that the Sandia tool does not account for screening by a landform. The shape of the GGZ is characterised by the times during the day when glint effects can occur.

There is potential for glint in the zone extending to the west when the sun is low in the sky and rising in the east, and conversely there is potential glint in the zone to the east when the sun is low in the sky as it is setting in the west. If a landform would prohibit sunlight from reaching the panel when it is at a low altitude the model would not necessarily account for this and suggest glint is visible when it is not

In summary although there are some limitations to the techniques used in this methodology, as the limitations are known they can be accounted for during the analysis. The techniques chosen in this report will still enable a robust and accurate assessment of potential glint effects.